Urban damage assessment using multimodal QuickBird images and ancillary data: the Bam and the Boumerdes earthquakes

Anne-Lise Chesnel, Renaud Binet, Lucien Wald

▶ To cite this version:

HAL Id: hal-00464847

https://hal-mines-paristech.archives-ouvertes.fr/hal-00464847

Submitted on 18 Mar 2010

Urban damage assessment using multimodal QuickBird images and ancillary data: the Bam and the Boumerdes earthquakes

Anne-Lise Chesnel and Renaud Binet
Commissariat à l'Energie Atomique
Département Analyse et Surveillance de l'Environnement
Bruyères-le-Châtel, 91297 Arpajon cedex, France
Email: annelise.chesnel@gmail.com, renaud.binet@cea.fr

Lucien Wald
Ecole des Mines de Paris
Centre Energétique et Procédés
06904 Sophia-Antipolis, France
Email: lucien.wald@ensmp.fr

Abstract— Remote sensing has proved its usefulness for the crisis mitigation through situation report and damage assessment. Visual analysis of satellite images is conducted by analysts, however automatic or decision aid method are desired. We propose a semi-automatic damage assessment method based on a pair of very high spatial resolution (VHR) images and some ancillary data. It is applied to two disaster cases, for which the QuickBird images acquisition conditions differ. For each case, the two images also have very different viewing and illumination angles. Hence their comparison requires a preliminary registration; an automatic method adapted to VHR images is described. Then several change features are extracted from the buildings, and their relevance to assess damage on buildings is evaluated. Some textural features allow a damage assessment, but correlation coefficients are more efficient. Finally, a step toward the full automation of the method is done, skipping the supervision step of the classification process. We show the robustness of the global approach for both disaster cases with average performances closed to 75 % when 4 damage classes are discriminated, up to 90 % for a intact/damaged detection.

I. INTRODUCTION

Major disasters across the world are more and more reported because their impact in terms of human and economical losses is increasing. This increase is explained by the growing population and by its migration in areas that are prone to disasters like seacoasts. Remote sensing has proved its usefulness for the crisis mitigation through situation report and damage assessment, as acknowledged by creation of initiatives like the International Charter *Space and Major Disaster* [1] or UN-OSAT [2]. In this operational scope, the required information is manually extracted from images acquired by satellites. Usually a reference image acquired before the disaster and a crisis image acquired after the disaster are visually compared to retrieve damage. Concerning damage assessment on buildings, Very High Resolution (VHR) images are usually used because they allow a more reliable visual analysis at this scale. The production of information has to be as short as possible, hence the need of automation to speed it up. Automatic methods for damage assessment are most of the time based on change detection methods. The most common applied method used to be pixel-based ones, like difference or ratio of images.

Recently, the improvement in spatial resolution of the remote sensing images leads to a widespread use of object oriented methods, e.g. post-classification comparisons. Some reviews of the principal methods can be found in [3]–[8]. Whatever the change detection method that is used, the images are to be made comparable, i.e. registered. This requirement is by fare acute when considering an automatic image analysis method.

On one hand, the crisis image has to be acquired as soon as possible following the disaster, regardless to the sensor type and the acquisition parameters; on the other hand, the reference image has to be as recent as possible, to avoid additional major changes that are not related to damage. Hence there is little chance for the crisis image to be acquired in the same conditions (acquisition angles for example), or even with the same sensor, than the reference image.

Moreover, the multitemporal analysis of VHR images exhibits more natural changes that are not related to damage [9]–[12]. This is for examples changes due to human activities, or shadow changes due to different illumination conditions. Another major source of changes is the difference in acquisition angles, the parallax effect leading to geometrical deformations. Theses natural changes have to be corrected or filtered out. All these differences represent a challenge for automatic images analysis methods. Object-oriented methods allow to focus the analysis on the objects of interest, thus to partly avoid false alarms due to natural changes. We focus on the buildings, more precisely on their roofs because they are most often visible by means of remote sensing. For this purpose, we use ancillary data that consist of the buildings roofs outlines in the reference image only. This data can be obtained after a disaster while waiting for the crisis image, by segmentation of the reference image or from a Geographical Information System.

We propose a method that allows a building damage assessment from a pair of images acquired in very different conditions (acquisition and illumination angles, season...). It is applied to two earthquake cases: the data are described in part II. An object oriented registration method is explained in part III-A and applied to retrieve the location of the buildings roofs in the crisis image that corresponds to each one in

the reference image. Then, as explained in part III-B, some change features are extracted from each building roof, to quantify the damage that may have occurred. The buildings are individually classified according to these features using a supervised classification tool. The figure 1 illustrates the main steps of the proposed method. The results are presented in part IV: the features that give the best performances are specified as a conclusion. Finally, the possibility to make our damage assessment approach automatic, skipping the supervised classification step, is considered in part V.
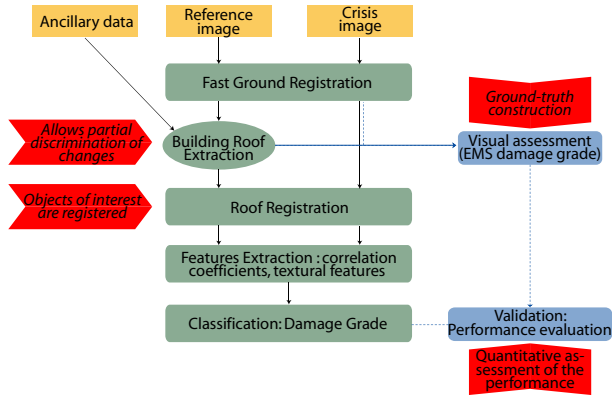

Fig. 1. Block diagram for damage assessment using a pair of panchromatic QuickBird images and ancillary data.

II. TEST-CASES AND DATABASES

The method is applied to two earthquake cases: the Bam (Iran) earthquake of December 26, 2003 and the Boumerdes (Algeria) earthquake of May 21, 2003. A pair of panchromatic QuickBird images is available for each disaster. The images have different illumination and acquisition parameters, that generate changes respectively in shadows and in image geometry. Three of the five damage grades of the European Macroseismic Scale (EMS) [13] can be discriminated at most by a visual analysis, leading to four-classes classification: intact, EMS3, EMS4 and EMS5. As ancillary data, the outlines of the buildings roofs have been manually extracted from the reference image.

A. Bam earthquake data

The reference image has been acquired September 30, 2003; the crisis image dated January 3, 2004. Some seasonal changes can be observed (vegetation, river), as long as some changes in illumination conditions. 2168 buildings have been extracted and are divided as follows: 475 intact buildings, 201 buildings are associated to the damage grade EMS3, 407 to the grade EMS4 and 1085 to the EMS5.

B. Boumerdes earthquake data

The reference image dated April 22, 2002; the crisis image has been acquired the May 23, 2003, the day after tomorrow the earthquake. Helped with an analysis presented in [14], we have conducted a visual analysis of the images to extract buildings and to associate a damage grade to each one. 610

buildings are extracted: 452 correspond to intact buildings, 77 to the EMS3, 16 to the EMS4 and 65 to the EMS5.

III. METHODOLOGY

A. Roofs registration

Using the ancillary data in agreement with the reference image, we propose a method that automatically searches for the buildings roofs outlines in the crisis image. It allows to compensate for the parallax, that is not negligible for the subsequent change analysis method. The correspondence of each roof in the crisis image is individually searched in a restricted area that is defined by the acquisition angles of both images; the greater the base to height ratio of the images pair, the larger the search area. This registration step is based on the joint maximization of two complementary correlation coefficients computed between the homologous pixels inside the buildings roofs outlines. The first is computed on the images and the second is obtained from the same images filtered by the Canny edge detector. The latter is particularly adapted in an urban context, due to the presence of multiple objects with different radiometry (buildings, roads, trees...). The former allow to discriminate for example edges due to shadows from building edges. Hence, the two correlation coefficients are complementary. For each location included in the search area, one compute a score that corresponds to the norm of the vector which coordinates are the two correlation coefficients. Its maximisation allows a fine subpixel registration of the building roofs.

The quality of the result of the fine registration step is a determining factor to the subsequent damage detection. An extract of the result is presented in figure 2: it shows the necessity to register specifically the buildings roofs (figure 2b) and the efficiency of the proposed registration method (figure 2c).

B. Damage assessment

1) Features extraction: The method attributes change co-efficients to each building by assessing the amount of change on their registered roofs. Two sets of object-oriented features are tested: one is based on correlation computed between the homologous pixels inside the buildings roofs, the other quantifies the change of texture of the buildings roofs.

The correlation coefficients used to quantify the damage correspond to the ones that have maximised the score during the registration step. These coefficients are sensitive to a non-linear change in the image radiometry. More specifically, the correlation coefficient computed on the images filtered by a Canny edge detector is sensitive to the partial or complete collapse of a building that leads to a change in the roof morphology. A building collapse also leads to a disappearance of the building shadow, and so to weaker or even to a lack of roof edge.

To characterize the texture, a set of anisotropic Gabor filters is defined [15], [16]. En illustration of this type of Gabor filter is given in figure 3 in the spatial domain and the corresponding filter in the frequency domain is given in figure 4. Their
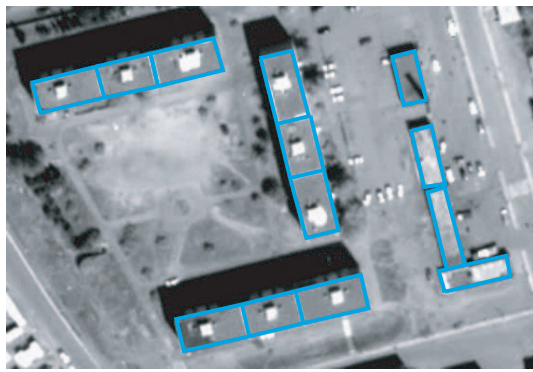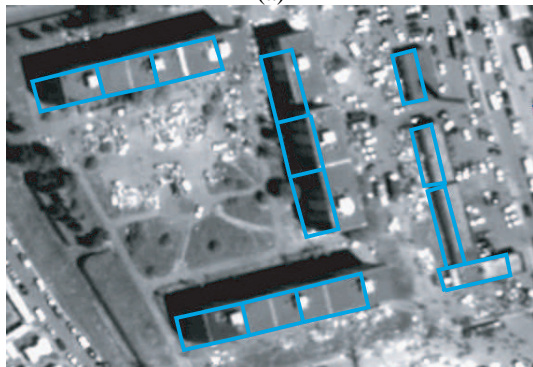
Fig. 2. Result of the registration step – case of Boumerdes. (a): reference image and ancillary data. – (b): crisis image registered to the reference image according to the ground, and buildings outlines reported using geographical coordinates. The buildings outlines are clearly shifted proportionally to the building height, preventing a comparison of the images. – (c): crisis image and automatically registered buildings outlines.

equation in the spatial domain is defined as followed:

$$f(c, l) = g(c, l) \exp\left(-2\pi j F \sqrt{c^2 + l^2}\right), \qquad (1)$$

$$\text{where } g(c, l) = \frac{1}{2\pi\sigma^2} \exp\left(-\frac{c^2 + l^2}{2\sigma^2}\right),$$

and F is the centre frequency. The scale factor σ is defined so that the high frequencies are more localised in space:

$$\sigma = \mu/F, \text{ where } \mu \text{ is constant.} \qquad (2)$$

A set of 13 filters is defined, with respectively centre frequency: $F = 0.1, 0.2, \ldots, 1.2, 1.3$.

The reference and crisis images are filtered and the amplitude of the results is retrieved. For each filter, the ratio of the energies computed for the pixels inside each roof outline before and after the disaster quantifies the amount of change between the two dates.
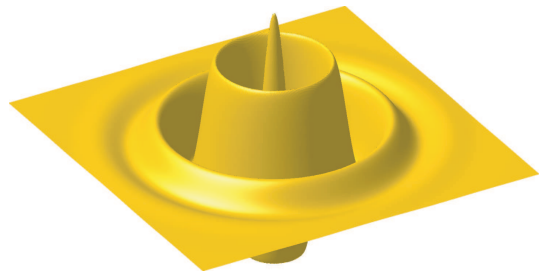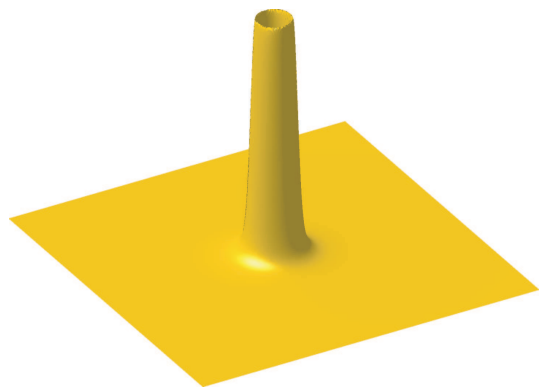

Fig. 3. Anisotrope Gabor filter in the spatial domain.

Fig. 4. Anisotrope Gabor filter in the Fourier domain.

2) Building classification: From these features, the buildings are individually classified to quantify damage. A supervised classification based on SVM is chosen for its efficiency in terms of rapidity and performances. However, because the proposed method is to be used in an operational context, the required training set has to be as small as possible. SVM allows to reach good classification performance with a small training set composed of 5 samples per class.

To obtain a multiclasse classification, several binary classifications are made using a dichotomy method, through a decision tree. For example, an illustration in the case of a classification among four damage grades is proposed in figure 5: the decision is in this case the grade EMS4. Several different architecture of trees can be designed in the same manner.
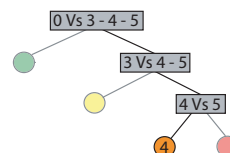

Fig. 5. Example of a decision tree used to obtain multiclasse classification from the SVM.

TABLE I

PERFORMANCES OF THE DAMAGE ASSESSMENT AS A FUNCTION OF THE
USED FEATURES.

	Test-case	
	Bam	Boumerds
13 textural features	64 %	60 %
Salient textural features	64 %	59 %
13 textural features + 2 correlation coeff.	71 %	64 %
Salient textural features + 2 correlation coeff.	76 %	64 %
2 correlation coeff. alone	78 %	74 %

IV. RESULTS

The effectiveness of the correlation coefficients and of the textural features is compared. A first classification is done using the 13 textural features; the dimension of the data being high and the size of the training being small, a second classification is made using only the two more discriminatory textural features (salient features). The results are gathered in table I.

We show that the textural features allow a discrimination of the four damage classes with a good classification from 59 % to 64 % of the buildings. Moreover, the correlation coefficients give better results, whatever the test-case: it improves the performances by about 15 %. Finally, the use of both features sets does not improve the results. We conclude that, although the textural features allow to a certain extent a damage assessment, it does not bring any additional information, comparing to the correlation coefficients alone.

Using only the correlation coefficients, we show that our method allows the identification of the 4 classes in the case of Bam with 78 % of good classification (figure 6); only three damage grades can be identified efficiently in the case of Boumerdes, the EMS3 being undetectable with our roof analysis approach (figure 7). Indeed, this damage grade corresponds in the case of Boumerdes to damage on the buildings walls; no change is observable on their roofs.

We assess the performance of the damage detection as a function of the number of distinguished damage levels. For both earthquake cases, the classification in three classes leads to an average performance equal to 75-80 %. Finally, when considering a two-classes problem, the performance increases up to 88 % in average. These results demonstrate that the proposed method is efficient and applicable to different damage types. Its performances are stable with different test-cases, except when damage are not structural and only affect the buildings walls. It explains the slight decrease of performances for the Boumerdes test-case. Moreover, the application of our method is fast and need a limited action of the image analyst.

V. GENERALIZATION CAPABILITY OF THE METHOD

Using a pair of VHR images and the ancillary data, the analysis of the images with the proposed method only requires an action of the operator during the classification step. A set of five buildings per class has been chosen. They are used to classify the whole buildings dataset. We investigate

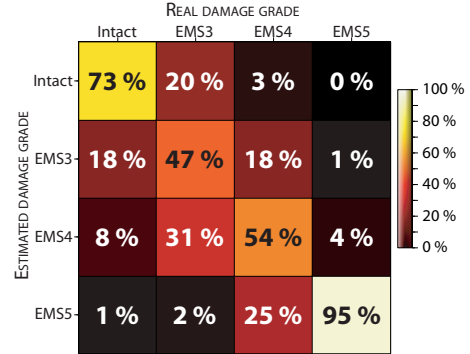|		Real damage grade			
		Intact	EMS3	EMS4	EMS5
Estimated damage grade	Intact	347	40	13	0
	EMS	87	95	71	7
	EMS4	38	62	220	50
	EMS5	3	4	103	1028
	Total	475	201	407	1085

Global performance: 78 %
Kappa Coefficient: 0.66

Fig. 6. Confusion matrix obtained from the classification of the buildings of Bam. Top: raw confusion matrix – Bottom: confusion matrix normalised per damage grade.

		Real damage grade			
		Intact	EMS3	EMS4	EMS5
Estimated damage grade	Intact	383	51	4	9
	EMS3	15	4	1	0
	EMS4	23	11	7	1
	EMS5	31	11	4	55
	Total	452	77	16	65

Global performance: 74 %
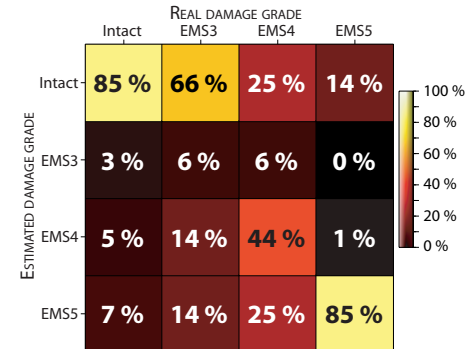Kappa Coefficient: 0.39

Fig. 7. Confusion matrix obtained from the classification of the buildings of Boumerdes. Top: raw confusion matrix – Bottom: confusion matrix normalised per damage grade.

the possibility to use a classifier trained with one test-case, to classify the buildings of another test-case. The results are shown in table III.

Comparing these results to the ones obtain with a specific training for each test-case (table II), we show a slight and limited decrease of the performance when the classifier is

TABLE II

CLASSIFICATION PERFORMANCE AS A FUNCTION OF THE NUMBER OF
DISCRIMINATED DAMAGE GRADE.

	Test-case	
	Bam	Boumerdes
4 classes	78 %	74 %
3 classes		
0-3-45	79 %	74 %
03-4-5	83 %	78 %
2 classes		
0-345	88 %	80 %
03-45	89 %	87 %

TABLE III

CLASSIFICATION PERFORMANCE AS A FUNCTION OF THE NUMBER OF
DISCRIMINATED DAMAGE GRADE.

	Test-case	
	Learning: Boumerdes Testing: Bam	Learning: Bam Testing: Boumerdes
4 classes	74 %	58 %
3 classes		
0-3-45	79 %	58 %
03-4-5	83 %	72 %
2 classes		
0-345	89 %	80 %
03-45	90 %	88 %

trained with another test-case when considering a four-classes classification. The classification among three classes gives almost equivalent results. Finally, the results of the damage detection (classification intact/damaged) are strictly equivalent in both cases. We show that the learning step could be skipped if necessary, making the method fully automatic. Moreover, if the number of damage grades to be distinguished is lower, the precision of the results would be exactly the same. These are promising results for a future operational application.

VI. CONCLUSION

We describe a building damage assessment method based on a pair of very high spatial resolution images and some ancillary data that contain the buildings footprints in the reference images. It has been applied to two disaster cases, in conditions that are close to an operational application. The images are acquired in realistic conditions (most recent reference image, first crisis image): they have different acquisition angle and exhibit changes in shadows and vegetation due to the difference in season. Moreover, the method is fast and closed to be fully automatic. It gives satisfactory results, particularly when the aim is to detect damaged buildings among intact ones.

To make our method fully automatic, we are currently working on the registration between real map/cadastre and a VHR image acquired with a high off-nadir angle. Future improvement would involve the extraction of buildings outlines directly from VHR images. Morphology based approaches seem promising and will be investigated.

REFERENCES

[1] International-Charter, "International charter *Space and Major Disasters*," 2007, available online at: http://www.disasterscharter.org/ (accessed 15 February 2007).

[2] UNOSAT, "United Nations Institute for Training and Research (UNITAR) Operational Satellite Applications Programme," 2007, available online at: http://unosat.web.cern.ch/ (accessed 2 August 2007).

[3] A. Singh, "Digital change detection techniques using remotely-sensed data," *International Journal of Remote Sensing*, vol. 10, no. 6, pp. 989–1003, 1989.

[4] D. Li, H. Sui, and P. Xiao, "Automatic change detection of geo-spatial data from imagery," in *Integrated System for Spatial Data Production, Custodian and Decision Support, (Xi'an, China), International Archives of Photogrammetry and Remote Sensing*, vol. 34, no. 2, August 2002.

[5] R. Radke, S. Andra, O. Al-Kofahi, and B. Roysam, "Image change detection algorithms: a systematic survey," *IEEE Transactions on Image Processing*, vol. 14, no. 3, pp. 294–307, March 2005.

[6] P. Deer, "Digital change detection techniques: Civilian and military applications," in *International Symposium for Spectral Sensing Research*, 1995.

[7] P. Coppin, I. Jonckheere, K. Nackaerts, B. Muys, , and E. Lambin, "Digital change detection methods in ecosystem monitoring: a review," *International Journal of Remote Sensing*, vol. 25, no. 9, pp. 1565–1596, May 2004.

[8] D. Lu, P. Mausel, E. Brondizio, and E. Moran, "Change detection techniques," *International Journal of Remote Sensing*, vol. 25, no. 12, pp. 2365–2407, June 2004.

[9] B. Adams, C. Huyck, B. Mansouri, R. Eguchi, and M. Shinozuka, "Application of high-resolution optical satellite imagery for post-earthquake damage assessment: The 2003 Boumerdes (Algeria) and Bam (Iran) earthquakes," *Research Progress and Accomplishments 2003-2004, Buffalo: MCEER*, 2004, available online at: http://mceer.buffalo.edu/publications/resaccom/04-SP01/12_Eguchi.pdf (accessed 15 February 2007).

[10] G. Bitelli, R. Camassi, L. Gusella, and A. Mongnol, "Image change detection on urban area: the earthquake case," in *XXth ISPRS Congress, Istanbul, Turkey*, July 2004, p. 692.

[11] Z. Chen and T. C. Hutchinson, "Urban damage estimation using statistical processing of satellite images: 2003 Bam, Iran earthquake," *Proceedings SPIE*, vol. 5667, pp. 289–300, 2005.

[12] M. Sakamoto, Y. Takasago, K. Uto, S. Kakumoto, Y. Kosugi, and T. Doihara, "Automatic detection of damaged area of Iran earthquake by high-resolution satellite imagery," in *IEEE Proceedings of International Geoscience and Remote Sensing Symposium 2004*, vol. 2, September 2004, pp. 1418–1421.

[13] G. Grünthal, R. Musson, J. Schwarz, and M. Stucchi, *L'Echelle Macrosismique Européenne 1998*. Cahiers du Centre Européen de Géodynamique et de Séismologie, Luxembourg, 2001, vol. 19.

[14] F. Yamazaki, K. Kouchi, M. Matsuoka, M. Kohiyama, and N. Muraoka, "Damage detection from high-resolution satellite images for the 2003 Boumerdes, Algeria earthquake," in *13th World Conference on Earthquake Engineering, International Association for Earthquake Engineering, Vancouver, British Columbia, Canada*, 2004, p. 13.

[15] J. Coggins and A. Jain, "A spatial filtering approach to texture analysis," *Pattern recognition letters*, vol. 3, no. 3, pp. 195–203, 1985.

[16] R. Porter and N. Canagarajah, "Robust rotation-invariant texture classification: wavelet, Gabor filter and GMRF based schemes," in *IEE Proceedings on Vision, Image and Signal Processing*, vol. 144, no. 3, June 1997, pp. 180–188.